Lock and Key Adsorption Chemistry: Preferential Absorption of an Isomer of Di-iodobenzene on Molecular Films of Quinonoid Zwitterions

ARTICLE *in* THE JOURNAL OF PHYSICAL CHEMISTRY C · JANUARY 2011

Impact Factor: 4.77 · DOI: 10.1021/jp110611u

8 AUTHORS, INCLUDING:

Lucie Routaboul
University of Strasbourg
33 PUBLICATIONS **484** CITATIONS
SEE PROFILE

Pierre Braunstein
University of Strasbourg
631 PUBLICATIONS **12,379** CITATIONS
SEE PROFILE

Bernard Doudin
University of Strasbourg
155 PUBLICATIONS **2,737** CITATIONS
SEE PROFILE

Peter Dowben
University of Nebraska at Lincoln
677 PUBLICATIONS **8,660** CITATIONS
SEE PROFILE

THE JOURNAL OF PHYSICAL CHEMISTRY C

ARTICLE

pubs.acs.org/JPCC

Lock and Key Adsorption Chemistry: Preferential Absorption of an Isomer of Di-iodobenzene on Molecular Films of Quinonoid Zwitterions

Zhengzheng Zhang,[†] Jose Alvira,[†,‡] Xenia Barbosa,[†,‡] Luis G. Rosa,[†,‡] Lucie Routaboul,[§] Pierre Braunstein,[*,§] Bernard Doudin,[*,∥] and Peter A. Dowben[*,†]

[†]Department of Physics, Astronomy, Nebraska Center for Materials, Nanoscience, University of Nebraska—Lincoln, Theodore Jorgensen Hall, 855 North 16th Street, Lincoln, Nebraska 68588, United States

[‡]Department of Physics, Electronics, University of Puerto Rico-Humacao, 100 Road 908 CUH Station, Humacao, PR 00791, and The Institute for Functional Nanomaterials, University of Puerto Rico, Facundo Bueso Building, Rio Piedras, PR 00931

[§]Laboratoire de Chimie de Coordination, Institut de Chimie (UMR 7177 CNRS), Université de Strasbourg, 4 rue Blaise Pascal, 67081 Strasbourg, France

[∥]Institut de Physique et Chimie des Matériaux de Strasbourg, IPCMS (UMR 7504), Université de Strasbourg, 23 rue du Loess B.P. 43, 67034 Strasbourg, France

ABSTRACT: We have investigated the absorption and adsorption of three isomers of di-iodobenzene on molecular films of a zwitterionic *p*-benzoquinonemonoimine-type molecule which is characterized by a large intrinsic dipole of 10 D. Specifically, we compared the reversible adsorption and absorption of 1,2-di-iodobenzene, 1,3-di-iodobenzene, and 1,4-di-iodobenzene on molecular films of (6*Z*)-4-(butylamino)-6-(butyliminio)-3-oxocyclohexa-1,4-dien-1-olate $C_6H_2(\cdots NHR)_2(\cdots O)_2$ where R = *n*-C_4H_9. We provide unequivocal evidence that molecular adsorption and absorption of 1,3-di-iodobenzene are strongly favored at 150 K over that of the other isomers of di-iodobenzene.

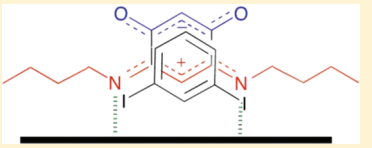

INTRODUCTION

Molecules possessing a strong intrinsic dipole can be used for testing if electrostatic dipolar interactions can lead to preferential adsorption on electrostatically biased substrates.[1−27] Both the magnitude of the molecular electrostatic dipole and the frontier orbital symmetry play a dominant role in the adsorption process. Even when intermolecular interactions do not involve any irreversible chemical reaction between the molecular species, there is a balance between the chemical interactions and the electrostatic dipolar interactions.[1,2,9−26]

Insight into these problems can be gained by comparing adsorption of isomeric molecules. The investigation of molecular isomeric effects in surface science is documented,[28−49] with most of the emphasis involving chiral surfaces[28−35] or chiral molecules. Isomer-specific surface chemistry has generally not been an emphasis in the study of molecular adsorbates on molecular substrates. Electrostatic interactions have often been implicated as the origin of the isomer-dependent chemistry,[36−42] and while the surface structures tend to depend on the isomer (often a chiral isomer), the adsorption process itself has not been conclusively demonstrated to be isomer-dependent. Of course, humans can distinguish between the smell of lemons and oranges (stereoisomers of limonene) or, perhaps more appropriately, the different isomers of the purine alkaloids dimethylated xanthines of theobromine (found in cacao), paraxanthine (the human metabolite of caffeine, found in coffee), and theophylline (found in tea). However, such an observation of molecular recognition of one isomer of a small molecule has rarely been seen in a reversible chemisorption experiment from the vapor.

Here we investigate di-iodobenzene adsorption/absorption on molecular films made of small, highly dipolar molecules, from the family of *p*-benzoquinonemonoimine zwitterions, with rather high symmetry properties, whose orientation and configuration when assembled as thin films on a gold surface have been recently investigated.[50] The zwitterionic molecule (6*Z*)-4-(butylamino)-6-(butyliminio)-3-oxocyclohexa-1,4-dien-1-olate, shown in Figure 1, is a small quinonoid molecule exhibiting a large intrinsic dipole of ca. 10 D magnitude.[51,52] This *p*-benzoquinonemonoimine zwitterion interacts with a gold substrate through the trimethyne cyanine part (cationic part) and adopts a preferential molecular orientation that places the zwitterion C_6 core parallel with the surface normal and the alkyl pendant groups parallel with the surface.[50] They form closed packed thin films, exempt of pinholes, that provide therefore a model electrostatically biased substrate, made of stacked dipoles perpendicular to the substrate plane.

At 150 K, the initial adsorption of all three isomers of di-iodobenzene is found to be similar on a conducting but chemically fairly inert substrate like graphite,[49] although a number of isomer-specific effects have been identified for the halogenated and substituted benzene adsorbates on surfaces.[48,49] Such small

Received: November 5, 2010
Revised: December 29, 2010
Published: January 21, 2011

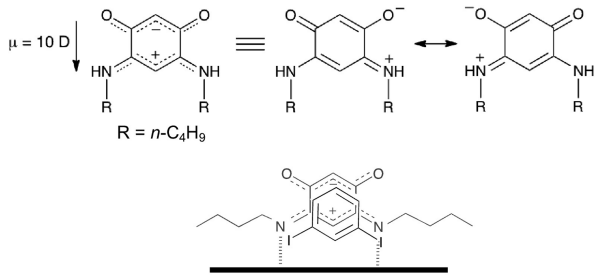

Figure 1. Molecular film substrate of this study, (6*Z*)-4-(butylamino)-6-(butyliminio)-3-oxocyclohexa-1,4-dien-1-olate $C_6H_2(\underline{\cdots}NHR)_2(\underline{\cdots}O)_2$, where R = n-C_4H_9, indicating the resonance structures involving the cationic nitrogen iminium and enamine functional groups and the anionic oxygen enolate and ketonic groups, respectively. The likely orientation and arrangement of the zwitterion, adapted from ref 50, are indicated at the bottom together with 1,3-di-iodobenzene.

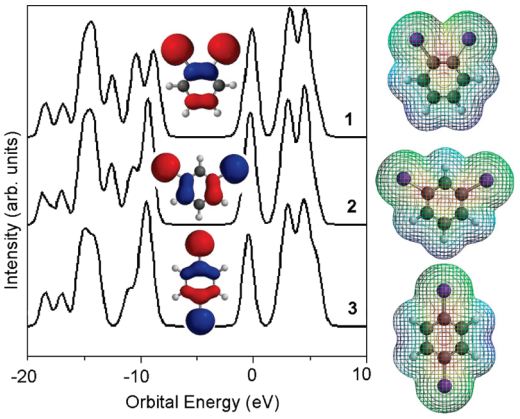

Figure 2. Model calculations of the (**1**) 1,2-di-iodobenzene, (**2**) 1,3-di-iodobenzene, and (**3**) 1,4-di-iodobenzene density of states obtained by applying equal Gaussian envelopes of 1 eV (black thin line) full width half-maximum to each molecular orbital to account for the solid state broadening in photoemission and then summing but uncorrected for matrix elements and final state effects. The calculated molecular orbitals are shown as a function of orbital energy and are not referenced to any Fermi level. Also shown are the schematics of the highest occupied molecular orbital (HOMO) of each di-iodobenzene, placed between the occupied (left) and unoccupied (right) molecular orbitals. Also shown are schematic representations of the charge densities based on Mulliken charge populations.

simple molecules provide a clear test of preferential isomer adsorption, particularly because their intrinsic dipole depends on the isomer: the dipole moment 1,2-di-iodobenzene is the largest with an experimentally determined value of 1.87 D[53] (1.856 D from density functional theory, with the PW91 exchange and correlation potential), while 1,3-di-iodobenzene is intermediate with a static dipole value of 1.19 D[53] (1.297 D from density functional theory), and of course 1,4-di-iodobenzene has a zero net dipole moment. These different charge distributions are schematically illustrated in Figure 2. It is, however, 1,3-disubstituted benzene that shares the same symmetry as the C_6 core of the zwitterion substrate molecules. While molecular dipoles certainly have a profound influence on adsorption,[1−27,54−61] here we show that dipolar interactions alone cannot explain the preferential adsorption of one isomer of di-iodobenzene. The oxygen and nitrogen functional groups of this class of *p*-benzoquinonemonoimine zwitterions should also play a role, as potentially influencing the chemoselective adsorption chemistry of a "guest" molecule from the vapor.[51,52,57]

EXPERIMENTAL SECTION

The zwitterion (6*Z*)-4-(butylamino)-6-(butyliminio)-3-oxocyclohexa-1,4-dien-1-olate, of formula $C_6H_2(\underline{\cdots}NHR)_2(\underline{\cdots}O)_2$ where R = n-C_4H_9 (**1**), was synthesized according to established procedures.[51,52,62,63] This zwitterion was deposited on clean gold substrates from a CH_2Cl_2 solution. A typical overnight exposure to a 0.8 mmol solution (0.2 g/L) was followed by extensive washing with ethanol to remove the excess molecules not bonded to the Au substrate.[50] Samples were dried and kept under a nitrogen atmosphere. Our measurements established that this "washing" procedure left a very thin, 0.5−1 nm thick, adsorbed molecular film covering the whole substrate (i.e., no pinholes). The film thickness was estimated from the attenuation of the substrate gold core level signal and independently confirmed by atomic force microscopy and quartz crystal microbalance (QCM) experiments. Films 2−3 nm thick were obtained by dipping the substrates into a more concentrated solution of the molecules, or by ethanol washing of the surface for much shorter times (ca. 1 min). Both methods provided similar pinhole-free molecular films, as described elsewhere.[50]

Combined photoemission and inverse photoemission spectra (IPES)[9−11,13,14,50,64−70] were taken of the *p*-benzoquinonemonoimine zwitterion (Figure 2) on gold, for molecular coverages that range from nominally 0.5 nm to the thicker multilayer films.[50] The ultraviolet photoemission (UPS) and inverse photoemission (IPES) spectra were taken in a single ultrahigh vacuum chamber to study the placement of both occupied and unoccupied molecular orbitals of the combined zwitterion−di-iodobenzene molecular systems as a function of di-iodobenzene exposure to the samples at 150 K. The IPES spectra were obtained by using variable kinetic energy electrons while detecting the emitted photons at a fixed energy (9.7 eV) using a Geiger−Müller detector.[9−11,13,14,28,50,64−72] The inverse photoemission spectroscopy was limited by an instrumental line width of approximately 400 meV, as described elsewhere.[28−31] The angle integrated photoemission (UPS) studies were carried out using a helium lamp at $h\nu$ = 21.2 eV (He I) and a Phi hemispherical electron analyzer with an angular acceptance of ±10° or more, as described in detail elsewhere.[9,10,64,66−69] The core level X-ray photoemission spectra were taken using a SPECS X-ray source with a Mg anode ($h\nu$ = 1253.6 eV). The photoemission experiments were made with the photoelectrons collected along the surface normal, while the inverse photoemission spectra were taken with the incident electrons normal to the surface. We performed the combined photoemission and inverse photoemission experiments with the electron emission (photoemission) or electron incidence (inverse photoemission) along the surface normal to preserve the highest point group symmetry and eliminate any wave vector component parallel with the surface. In both the photoemission and inverse photoemission measurements, the binding energies are referenced with respect to the Fermi edge of gold in intimate contact with the sample surface, and the photoemission (UPS, XPS) data are expressed in terms of $E - E_F$ (thus making occupied state energies negative).

The studies were carried out at 150 K, well below the expected desorption temperature of the di-iodobenzenes.[49] Although we do note that while all three isomers of di-iodobenzene will adsorb

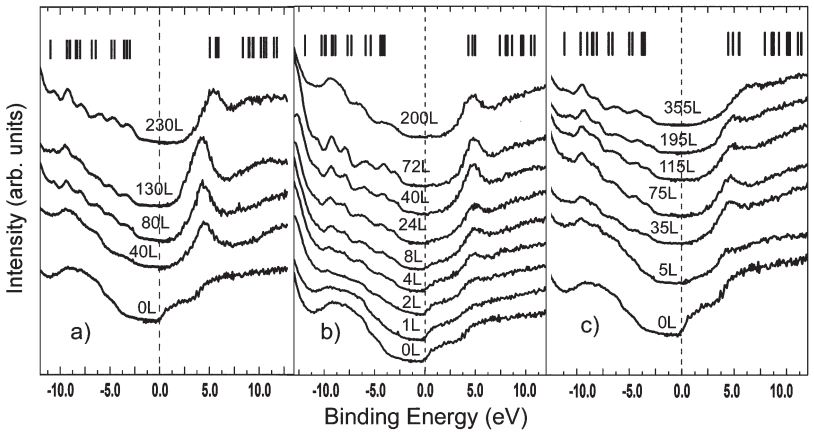

Figure 3. Combined photoemission and inverse photoemission of 1 nm thick *p*-benzoquinonemonoimine zwitterion molecular films as a function of (a) 1,2-di-iodobenzene, (b) 1,3-di-iodobenzene, and (c) 1,4-di-iodobenzene exposure. The exposures were done with the *p*-benzoquinonemonoimine zwitterion molecular films maintained at 150 K, and exposure is denoted in Langmuirs (L), where 1 L = 1×10^{-6} Torr s. The bars at the top of each panel are the placement of the molecular orbitals rigidly shifted about 5 eV, approximately consistent with the work function. Binding energies are in terms of $E - E_F$.

on the ferroelectric copolymer polyvinylidene (70%) with trifluoroethylene (30%) (PVDF-TrFE) at 150 K, at 160 K, 1,2-di-iodobenzene and 1,3-di-iodobenzene do not readily adsorb on PVDF-TrFE, while 1,4-di-iodobenzene will absorb. Each isomer of di-iodobenzene (Sigma-Aldrich >99% purity for 1,2-di-iodobenzene and 1,4-di-iodobenzene; >98% purity for 1,3-di-iodobenzene) was admitted to the vacuum chamber through a standard leak valve and thus absorbed or adsorbed on the zwitterion molecular films from the vapor. Exposures are denoted in Langmuirs (L), where 1 L = 1×10^{-6} Torr s. We believe that there is some photodecomposition because after many (10−20) cycles of absorption/adsorption at 150 K followed by extensive photoemission studies, and desorption at or below 300 K, a trace signal of the iodine 3d core level can be observed at room temperature. Samples were therefore routinely replaced after a maximum of a few cycles, to avoid any contribution from di-iodobenzene fragment contamination as a result of this photodissociation common to many halogenated benzenes.

Adsorption of Di-iodobenzene on *p*-Benzoquinonemonoimine Zwitterion Molecular Films. All three isomers of di-iodobenzene adsorb molecularly on 0.5−1 nm thick films of *p*-benzoquinonemonoimine zwitterion (of Figure 1), with the substrates held at 150 K. The characteristic molecular orbitals of 1,2-di-iodobenzene, 1,3-di-iodobenzene, and 1,4-di-iodobenzene are clearly evident in the combined photoemission and inverse photoemission spectra, shown in Figure 3 for zwitterion molecular films of identical thickness and preparation. There is, however, no indication of interactions of any of the di-iodobenzenes with the underlying Au substrate, confirming previous observations on clean graphite[49] and copper surfaces.[47]

The combined photoemission and inverse photoemission spectra of the *p*-benzoquinonemonoimine zwitterion molecular films on Au indicate a highest occupied molecular orbital (HOMO) to lowest unoccupied molecular orbital (LUMO) gap of 5.8−6.0 eV for the thinner of the films. These experimental values are consistent with the calculated value of 5.8 eV based on the simplistic single molecule semiempirical method NDO-PM3 (neglect of differential diatomic overlap, parametric model number 3), as discussed in detail elsewhere.[50]

With increasing exposure of all three isomers of di-iodobenzene, the apparent HOMO−LUMO gap increases, and features appear in the spectra (Figure 3) consistent with the molecular orbitals of the pertinent di-iodobenzenes, as seen in Figure 2. There is agreement of the single molecule calculations with the combined photoemission and inverse photoemission, as seen in Figure 3. Good agreement is found between the observed (Figure 3) and calculated (Figure 2 and top of Figure 3) levels of the molecular orbitals of the di-iodobenzenes. In fact, the various isomers of di-iodobenzene actually have a very similar electronic structure, as illustrated in Figure 2, where the calculated density of states (DOS) was obtained by applying equal Gaussian envelopes of 1 eV full width half-maximum to each molecular orbital, to account for the solid state broadening in photoemission, and then summing. There should be differences from expectations based on a single molecule and a thin film due to intermolecular interactions within the film (solid state effects) and band structure, and the model PM3 is a simplistic semiempirical single molecule ground state calculation not corrected for matrix element effects. Such comparisons with experiments are nevertheless often successful,[9−14,50,56,64,65,68,69] as seen here, although the calculated orbital energies must be rigidly shifted in energy by about 5 eV, largely to account for the influence of work function.

The adsorption of all of the di-iodobenzenes on the *p*-benzoquinonemonoimine zwitterion molecular films is seen to be reversible with no characteristic molecular orbitals nor any iodine 3d core level signal evident upon annealing to room temperature. There are clear experimental indications that the isomers, while all adsorbing on the zwitterion molecular films, exhibit isomeric dependence. The exposure-dependent spectra of Figure 3 reveal that the spectral features corresponding to the signature of di-iodobenzene molecular orbitals appear at exposure values depending on the isomer. The 1,2-di-iodobenzene requires 60−80 L exposure to approximately 1 nm thick *p*-benzoquinonemonoimine zwitterion molecular films at 150 K; the 1,4-di-iodobenzene requires some 10−15 L exposure; and the 1,3-di-iodobenzene requires only about 4 L exposure for the molecular orbitals to become evident in the combined photoemission and inverse photoemission spectra. Extending these observations to a

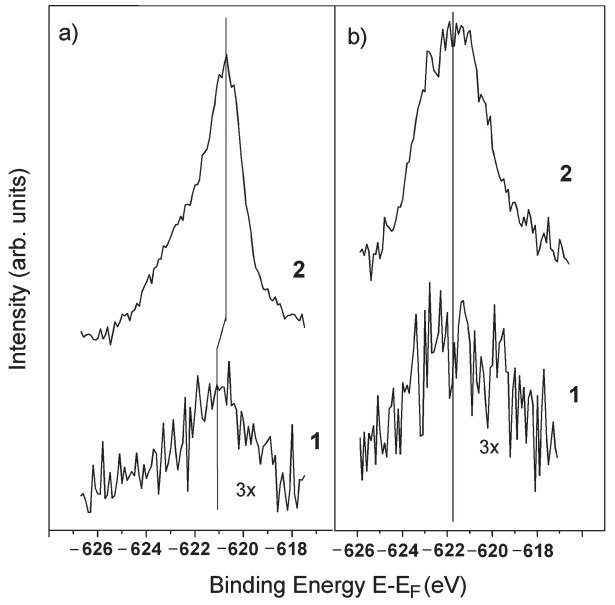

Figure 4. $3d_{5/2}$ iodine core level spectra following (a) 1,2-di-iodobenzene adsorption (1, 5 L exposure; 2, 600 L exposure) and (b) 1,4-di-iodobenzene adsorption (1, 250 L exposure; 2, 1200 L exposure) to zwitterion molecular films of identical 3 nm thickness and preparation. Binding energies are in terms of $E - E_F$.

coverage dependence on the isomer requires introducing the sticking coefficients S, assuming a linear relation between the exposure x and coverage y

$$y = \frac{S}{q}\left(\frac{x}{x_0}\right)$$

where x_0 is the exposure needed to form one monolayer of coverage (roughly 8×10^{18} molecules/m^2) and q is the ratio of adsorbate ionization cross section to that of N_2, neither established here. We may assume that the ionization gauge cross sections of all of the di-iodobenzenes are likely much higher than for nitrogen; for example, the toluene ionization gauge cross-section is 6.4 times greater than nitrogen,[73] while it is a factor of 3.5[73] to 5.7[74] greater for benzene than nitrogen. Furthermore, one can reasonably assume that the ionization gauge cross section of each of the di-iodobenzenes is in fact similar, as has been assumed elsewhere.[49] We therefore infer that the sticking coefficient of 1,3-di-iodobenzene on *p*-benzoquinonemonoimine zwitterion molecular films is roughly 3−5 times larger than that observed for 1,4-di-iodobenzene and 15 times larger than for 1,2-di-iodobenzene adsorption at 150 K. This qualitative trend is even more apparent on thicker (2−3 nm thick) *p*-benzoquinonemonoimine zwitterion molecular films at 150 K, as detailed in the next section.

Isomeric Dependence of the Di-iodobenzene Adsorption on *p*-Benzoquinonemonoimine Zwitterion Molecular Films. Another approach to investigating the preferential adsorption and absorption of one particular isomer of di-iodobenzene is to look at the increase in the core level iodine signals with exposure time. This type of experiment was performed on thicker *p*-benzoquinonemonoimine zwitterion films, approximately 2−3 nm thick. As seen in Figure 4, significant exposures of 1,2-di-iodobenzene and 1,4-di-iodobenzene to thick *p*-benzoquinonemonoimine zwitterion molecular films at 150 K are necessary for appreciable iodine $3d_{5/2}$ core level signals. This is in strong

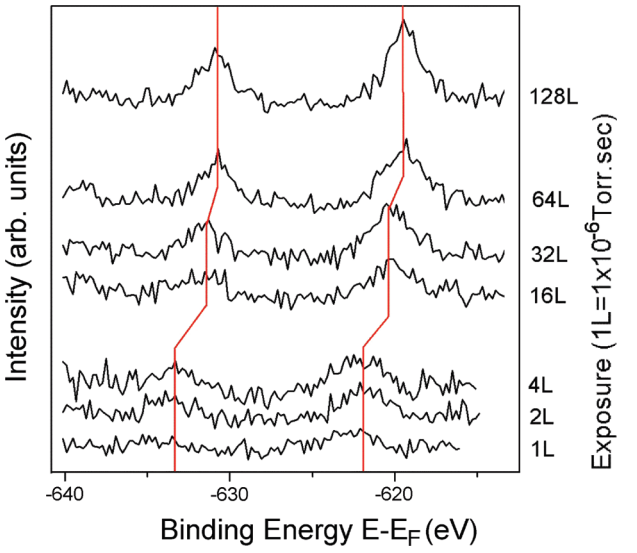

Figure 5. X-ray photoemission spectra for I 3d core levels of 1,3-di-iodobenzene adsorbed on 3 nm *p*-benzoquinonemonoimine zwitterion molecular films at 150 K. The core level binding energy shifts of both the I $3d_{5/2}$ and I $3d_{3/2}$ peaks are indicated by vertical bars (see text).

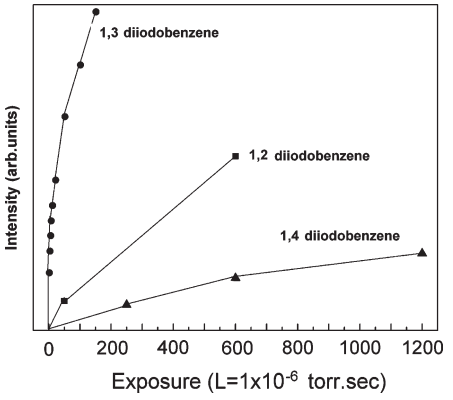

Figure 6. Iodine $3d_{5/2}$ core level intensities with increasing exposure of (■) 1,2-di-iodobenzene, (●) 1,3-di-iodobenzene, and (▲) 1,4-di-iodobenzene exposures to 3 nm thick *p*-benzoquinonemonoimine zwitterion molecular films maintained at 150 K. Exposures are denoted in Langmuirs (L), were 1 L = 1×10^{-6} Torr s.

contrast with iodine signals of 1,3-di-iodobenzene adsorption/absorption, which is remarkably more efficient, as seen in Figure 5. The iodine $3d_{5/2}$ X-ray photoemission core level signal for 1,3-di-iodobenzene is roughly 70 times larger than observed for 1,2-di-iodobenzene and 210−250 times larger than observed for 1,4-di-iodobenzene, using in all cases thick *p*-benzoquinonemonoimine zwitterion molecular films at 150 K, as summarized in Figure 6. Again, we see a strong preference for the adsorption/absorption of 1,3-di-iodobenzene.

The 1,3-di-iodobenzene exposure-dependent XPS spectra show very large shifts in the I 3d core level binding energies, as evident in Figure 5. These increases in core level binding energies of ∼2.5 eV or more are far greater than observed for 1,2- and 1,4-di-iodobenzene (Figure 4). Since dissociative chemisorption can be excluded in all data of the adsorption systems we describe here, such large core level shifts should result from strong intermolecular interactions or from decreased screening from the substrate with

dx.doi.org/10.1021/jp110611u |*J. Phys. Chem. C* 2011, 115, 2812–2818

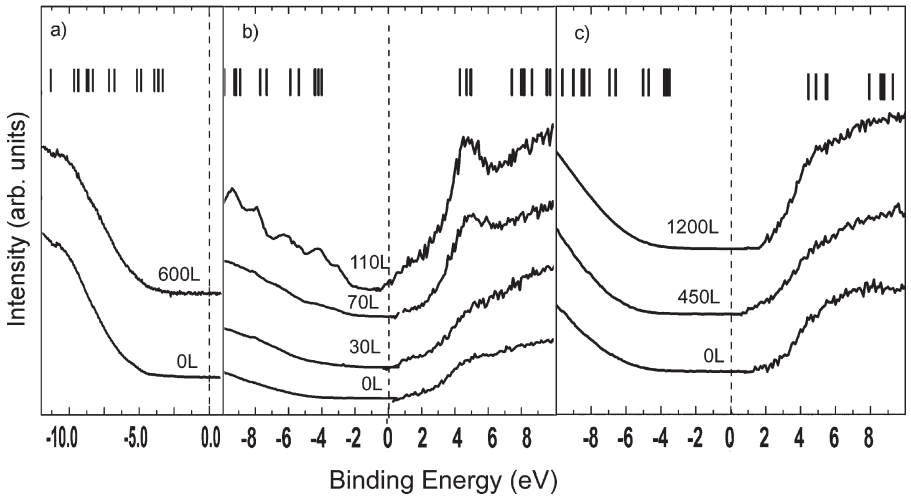

Figure 7. Combined photoemission and inverse photoemission of *p*-benzoquinonemonoimine zwitterion molecular films as a function of (a) 1,2-di-iodobenzene, (b) 1,3-di-iodobenzene, and (c) 1,4-di-iodobenzene exposure. The *p*-benzoquinonemonoimine zwitterion molecular films, of identical 3 nm thickness and preparation, were maintained at 150 K, and exposure is denoted in Langmuirs (L), were 1 L = 1×10^{-6} Torr s. The bars at the top of each panel are the placement of the di-iodobenzene molecular orbitals rigidly shifted about 5 eV, approximately consistent with the work function. Binding energies are in terms of $E - E_F$.

increasing di-iodobenzene film thickness,[49] resulting in larger photoemission final state binding energies.[10,75−77] Both effects would lead to energy shifts, but such final state effects should lead to a decrease,[77−79] not an increase, in core level binding energies with increasing di-iodobenzene coverages.[49] Changes in the final state screening,[75−77] with increasing di-idodobenzene coverages, also tend to be excluded because there is no change in the HOMO−LUMO gap of the adsorbed 1,3-di-iodobenzenes, as seen in Figures 3 and 7.

Excluding final state effects, and molecular dissociation, the shifts observed in the I 3d core level shift with increasing 1,3-di-iodobenzene coverage can also originate from two different species: an absorbed phase of di-iodobenzene within the *p*-benzoquinonemonoimine zwitterion molecular films and an adsorbed phase, near or at the surface of the *p*-benzoquinonemonoimine zwitterion molecular films. With increasing exposure to di-iodobenzene, the X-ray photoemission iodine signals appear well before the molecular orbital peaks appear in the combined photoemission and inverse photoemission spectra of Figure 7. The larger probing depth for the iodine $3d_{5/2}$ core level photoemission feature is a result of the different electron mean free paths through the molecular film with the different electron spectroscopies. The different probing depths are related to significantly greater electron kinetic energies (633 eV) in XPS than the valence band photoemission (16 eV), with inverse photoemission being notoriously even more surface sensitive.[80,81] The I 3d core level feature may be therefore representative of an absorbed phase of 1,3-di-iodobenzene. It is only with the largest di-iodobenzene exposure values where sites in the vicinity or at the surface become populated and become evident in inverse photoemission and the low(er) photon energy valence band photoemission.

Accordingly, we can partially attribute these different I $3d_{5/2}$ core level binding energies to the differences between absorbed (621.9 ± 0.2 eV) and adsorbed (619.4 ± 0.4 eV) 1,3-di-iodobenzene. The initial iodine $3d_{5/2}$ core level binding energies for 1,3-di-iodobenzene (621.9 ± 0.2 eV), 1,2-di-iodobenzene (621.1 ± 0.4 eV), and 1,4-di-idobenzene (621.7 ± 0.4 eV) are significantly greater than the binding energy of 620.7 ± 0.1 eV observed for the initial molecular adsorption of all three isomers on graphite[49] and 1,4-di-idobenzene adsorption on the ferroelectric copolymer polyvinylidene (70%) with trifluoroethylene (30%) with a binding energy value of 620.8 ± 0.2 eV. While adsorption on a semimetal like graphite is difficult to compare to adsorption on a poorly conducting zwitterion film, the values obtained with dielectric ferroelectric copolymer polyvinylidene (70%) with trifluoroethylene (30%) should be similar if the intermolecular interactions are minimal. In any case, the change in the initial I $3d_{5/2}$ core level binding energy is toward smaller binding energies with increasing di-iodobenzene coverages on *p*-benzoquinonemonoimine zwitterion molecular films at 150 K, in contrast to di-iodobenzene adsorption on graphite.[49] The core level binding energies support the contention that there are strong intermolecular interactions between the di-idobenzenes and *p*-benzoquinonemonoimine zwitterion molecules, especially for 1,3-di-iodobenzene.

The far greater sticking coefficient and far larger core level binding energy shifts (I $3d_{5/2}$ decreasing from 621.9 ± 0.2 to 619.4 ± 0.1 eV) with increasing 1,3-di-iodobenzene coverages suggest that this isomer favors strong $\pi-\pi$ interactions with the adjacent *p*-benzoquinonemonoimine zwitterion molecules. The large iodine 3d core level shifts seen with 1,3-di-iodobenzene are also consistent with an absorbed phase of 1,3-di-iodobenzene followed by adsorption of a surface-related phase on the *p*-benzoquinonemonoimine zwitterion molecular film, with increasing exposure. Exposure of 1,2-di-iodobenzene and 1,4-di-iodobenzene to the 3 nm thick *p*-benzoquinonemonoimine zwitterion molecular films at 150 K does not provide signature of di-iodobenzene molecular orbitals in the combined photoemission and inverse photoemission, even with significant exposure of several hundreds of Langmuirs. As seen in Figure 7, the characteristic di-idobenzene molecular orbitals are only observed in the combined photoemission and inverse photoemission in the case of 1,3-di-iodobenzene exposure to thicker (3 nm thick) zwitterion molecular films. Given that there are clear indications of di-iodobenzene adsorption from the core level photoemission, we must conclude that 1,2-di-iodobenzene and 1,4-di-iodobenzene exposures (in the range studied here) have only led to absorption within the bulk of the thicker 3 nm *p*-benzoquinonemonoimine

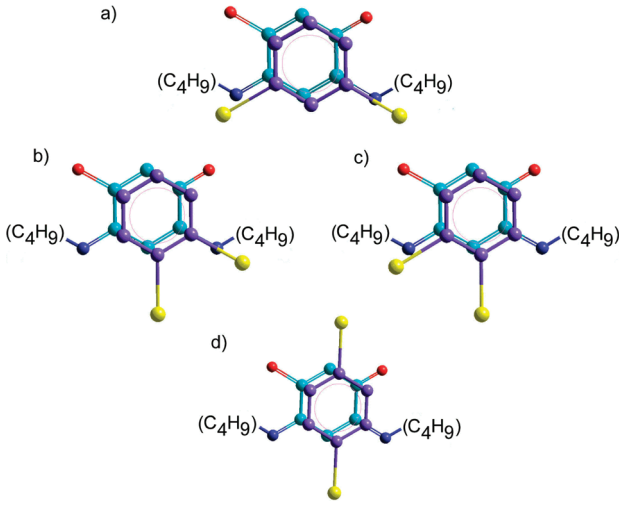

Figure 8. Lock and key configuration for the absorption interactions between the di-iodobenzene isomers and the *p*-benzoquinonemonoimine zwitterion: (a) 1,3-di-iodobenzene, (b), (c) 1,2-di-iodobenzene, (d) 1,4-di-iodobenzene. Color code: nitrogen (dark blue), carbon (light blue and violet), iodine (yellow), oxygen (red).

zwitterion molecular films at 150 K, with no surface or near surface adsorption sites occupied. This goes a long way toward explaining the smaller or negligible iodine X-ray photoemission core level shifts observed (Figure 3) for 1,2-di-iodobenzene and 1,4-di-iodobenzene.

These molecules are dielectrics, and even small core level shifts are not a good indication of future trends with continued di-iodobenzene adsorption. The XPS core level binding energies will not and should not saturate at a specific value. With extensive adsorption, as when a di-iodobenzene ice is formed at the surface, there are changes to the overall dielectric properties of the combined molecular film, and final state effects will then dominate the photoemission spectra.

SUMMARY

Di-iodobenzene adsorption studies on molecular films of the zwitterionic *p*-benzoquinonemonoimine compound C_6H_2-(···NHR)$_2$(···O)$_2$ where R = *n*-C_4H_9 reveal that 1,3-di-iodobenzene adsorption is strongly favored. This isomer of di-iodobenzene shares the same symmetry as the C_6 core of the *p*-benzoquinonemonoimine zwitterion compound, suggesting that the frontier molecular orbital symmetry plays a dominant role in preferential isomeric adsorption. Indeed, the highest occupied molecular orbital (HOMO) of 1,3-di-iodobenzene (Figure 2) bears considerable resemblance to the lowest unoccupied molecular orbital (LUMO) of the core of the *p*-benzoquinonemonoimine zwitterion compound. This molecular recognition phenomenon should therefore be understood within models going beyond simple dipolar interactions, as there are indications that the HOMO of 1,3-di-iodobenzene can strongly hybridize with the LUMO of this *p*-benzoquinonemonoimine zwitterion compound, if the relative orientation of Figure 8 is adopted.

It is clear that there is one orientation of 1,3-di-iodobenzene that favors strong $\pi-\pi$ interactions (see Figure 8), with a concomitant electric dipole coalignment with the adjacent *p*-benzoquinonemonoimine molecules. The two orientations of 1,2-di-iodobenzene that favor $\pi-\pi$ interactions are shown in Figure 8, with electric dipole coalignment, with the adjacent *p*-benzoquinonemonoimine molecules, but the alignment is imperfect and the symmetry not preserved. For 1,4-di-iodobenzene, there is one symmetry-preserving orientation that favors $\pi-\pi$ interactions with the adjacent *p*-benzoquinonemonoimine molecules, but apart from some induced dipole in the 1,4-di-iodobenzene, there is no expected real dipole alignment (see Figure 8). If the multiplicity of available favorable orientations based on dipole and $\pi-\pi$ interactions is the key factor determining preferential isomeric attachment, then absorption of 1,2-di-iodobenzene should be preferred, in contradiction with our experimental findings. Our experiments demonstrate that reversible isomer-selective adsorption chemistry of small molecules is indeed possible, with a preferential adsorption mechanism illustrating that symmetry does matter.

AUTHOR INFORMATION

Corresponding Author

*Tel.: +1-402-472-9838. Fax: +1-402-472-6148. E-mail: pdowben@unl.edu. Tel.: +33-(0)368851308. Fax: +33-(0)368851322. E mail: braunstein@unistra.fr.

ACKNOWLEDGMENT

This research was supported by the National Science Foundation through grant numbers CHE-0909580 and DMR-0851703, the Centre National de la Recherche Scientifique and the Ministère de la Recherche et des Nouvelles Technologies, the ANR (07-BLAN-0274-04), and the Nebraska Center for Materials and Nanoscience at University of Nebraska-Lincoln. The authors acknowledge the assistance of Gerson Díaz, Rosette González, and Xin Zhang with the di-iodobenzene adsorption experiments on PVDF-TrFE, Guillaume Dalmas and Victor DaCosta for complementary surface characterization experiments, and Dr. Roberto Pattacini for discussions.

REFERENCES

(1) Lvov, V. S.; Naaman, R.; Tiberkevich, V.; Vage, Z. *Chem. Phys. Lett.* **2003**, *381*, 650–653.
(2) Cahen, D.; Naaman, R.; Vager, Z. *Adv. Funct. Mater.* **2005**, *15*, 1571–1578.
(3) Duan, C. G.; Mei, W. N.; Yin, W. G.; Liu, J. J.; Hardy, J. R.; Ducharme, S.; Dowben, P. A. *Phys. Rev. B* **2004**, *69*, 235106.
(4) Kuehn, M.; Kliem, H. *Phys. Status Solidi B* **2008**, *245*, 213–223.
(5) Guo, W.; Du, S. X.; Zhang, Y. Y.; Hofer, W. A.; Seidel, C.; Chi, L. F.; Fuchs, H.; Gao, H.-J. *Surf. Sci.* **2009**, *603*, 2815–2819.
(6) Feng, M.; Gao, L.; Deng, Z.; Ji, W.; Guo, X.; Du, S.; Shi, D.; Zhang, D.; Zhu, D.; Gao, H. *J. Am. Chem. Soc.* **2007**, *129*, 2204–2205.
(7) Lewis, P. A.; Inman, C. E.; Maya, F.; Tour, J. M.; Hutchison, J. E.; Weiss, P. S. *J. Am. Chem. Soc.* **2005**, *127*, 17421–17426.
(8) Gao, H. J.; Sohlberg, K.; Xue, Z. Q.; Chen, H. Y.; Hou, S. M.; Ma, L. P.; Fang, X. W.; Pang, S. J.; Pennycook, S. J. *Phys. Rev. Lett.* **2000**, *84*, 1780–1783.
(9) Dowben, P. A.; Rosa, L. G.; Ilie, C. C.; Xiao, J. *J. Electron Spectrosc. Relat. Phenom.* **2009**, *174*, 10–21.
(10) Xiao, J.; Dowben, P. A. *J. Mater. Chem.* **2009**, *19*, 2172–2178.
(11) Xiao, J.; Sokolov, A.; Dowben, P. A. *Appl. Phys. Lett.* **2007**, *90*, 242907.
(12) Rosa, L. G.; Xiao, J.; Losovyj, Ya. B.; Gao, Y.; Yakovkin, I. N.; Zeng, X. C.; P.A. Dowben, P. A. *J. Am. Chem. Soc.* **2005**, *127*, 17261–17265.
(13) Rosa, L. G.; Jacobson, P. A.; Dowben, P. A. *J. Phys. Chem. B* **2006**, *110*, 7944–7950.

(14) Dowben, P. A.; Rosa, L. G.; Ilie, C. C. *Z. Phys. Chem.* **2008**, *222*, 755–778.
(15) Levshin, N. L.; Yudin, S. G.; Diankina, A. P. *Moscow Univ. Phys. Bull.* **1997**, *52*, 71–74.
(16) Levshin, N. L.; Yudin, S. G. *Vysokomol. Soedin., Ser. B* **2004**, *46*, 1981 (Eng. Transl.). Levshin, N. L.; Yudin, S. G. *Poly. Sci., Ser. B* **2004**, *46*, 348.
(17) Levshin, N. L.; Pestova, S. A.; Yudin, S. G. *Colloid J.* **2001**, *63*, 205.
(18) Yun, Y.; Altman, E. I. *J. Am. Chem. Soc.* **2007**, *129*, 15684.
(19) Garrity, K.; Kolpak, A. M.; Ismail-Beigi, S.; Altman, E. I. *Adv. Mater.* **2010**, *22*, 2969–2973.
(20) Yun, Y.; Kampschulte, L.; Li, M.; Liao, D.; Altman, E. I. *J. Phys. Chem. C* **2007**, *111*, 13951.
(21) Cabrera, A. L.; Tarrach, G.; Lagos, P.; Cabrera, G. B. *Ferroelectrics* **2002**, *281*, 53.
(22) Li, D.; Zhao, M. H.; Garra, J.; Kolpak, A. M.; Rappe, A. M.; Bonnell, D. A.; Vohs, J. M. *Nat. Mater.* **2008**, *7*, 473.
(23) Vohs, J. M.; Barteau, M. A. *J. Phys. Chem.* **1991**, *95*, 297–302.
(24) Zhao, M. H.; Bonnell, D. A.; Vohs, J. M. *Surf. Sci.* **2009**, *603*, 284.
(25) Garra, J.; Vohs, J. M.; Bonnell, D. A. *Surf. Sci.* **2009**, *603*, 1106.
(26) Zhao, M. H.; Bonnell, D. A.; Vohs, J. M. *Surf. Sci.* **2008**, *602*, 2849–2855.
(27) Zhang, Z.; Sharma, P.; Borca, C. N.; Dowben, P. A.; Gruverman, A. *Appl. Phys. Lett.* **2010**, *97*, 243702.
(28) Ahmadi, A.; Attard, G.; Feliu, J.; Rodes, A. *Langmuir* **1999**, *15*, 2420–2424.
(29) Gellman, A. J. *ACS Nano* **2010**, *4*, 5–10.
(30) Attard, G. A. *J. Phys. Chem. B* **2001**, *105*, 3158–3167.
(31) Sholl, D. S.; Gellman, A. J. *AIChE J.* **2009**, *55*, 2484–2490.
(32) Held, G.; Gladys, M. J. *Top. in Catal.* **2008**, *48*, 128–136.
(33) James, J. N.; Sholl, D. S. *Curr. Opin. Colloid Interface Sci.* **2008**, *13*, 60–64.
(34) Greber, T.; Sljivancanin, Z.; Schillinger, R.; Wider, J.; Hammer, B. *Phys. Rev. Lett.* **2006**, *96*, 056103.
(35) Kühnle, A.; Linderoth, T. R.; Besenbacher, F. *J. Am. Chem. Soc.* **2006**, *128*, 1076–1077.
(36) Blankenburg, S.; Schmidt, W. G. *Phys. Rev. Lett.* **2007**, *99*, 196107.
(37) Chen, Q.; Richardson, N. V. *Nat. Mater.* **2003**, *2*, 324–328.
(38) Kühnle, A.; Linderoth, T. R.; Hammer, B.; Besenbacher., F. *Nature* **2002**, *415*, 891–893.
(39) Santagata, N. M.; Lakhani, A. M.; Davis, B. F.; Luo, P.; Nardelli, M. B.; Pearl, T. P. *J. Phys. Chem. C* **2010**, *114*, 8917–8925.
(40) Graff, M.; Bukowska, J. *Vib. Spectrosc.* **2010**, *52*, 103–107.
(41) Bieri, M.; Burgi, T. *Chem. Phys. Chem.* **2006**, *7*, 514–523.
(42) De Feyter, S.; Gesquiere, A.; Wurst, K.; Amabilino, D. B.; Veciana, J.; De Schryver, F. C. *Angew. Chem., Int. Ed.* **2001**, *40*, 3217.
(43) Mondelli, C.; Vargas, A.; Santarossa, G.; Baiker, A. *J. Phys. Chem. C* **2009**, *113*, 15246–15259.
(44) Raval, R. *Chem. Soc. Rev.* **2009**, *38*, 707–721.
(45) Barlow, S. M.; Louafi, S.; Le Roux, D.; Williams, J.; Muryn, C.; Haq, S.; Raval, R. *Langmuir* **2004**, *20*, 7171–7176.
(46) Haq, S.; Liu, N.; Humblot, V.; Jansen, A. P. J.; Raval, R. *Nature Chem.* **2009**, *1*, 409–414.
(47) Kim, B. I. *Langmuir* **2006**, *22*, 9272–9280.
(48) Meyers, J. M.; Gellman, A. J. *Surf. Sci.* **1995**, *337*, 40.
(49) Fukutani, K.; Wu, N.; Dowben, P. A. *Surf. Sci.* **2009**, *603*, 2964–2971.
(50) Xiao, J.; Zhang, Z.-Z.; Wu, D.; Routaboul, L.; Braunstein, P.; Doudin, B.; Losovyj, Ya. B.; Kizilkaya, O.; Rosa, L. G.; Borca, C. N.; Gruverman, A.; Dowben, P. A. *Phys. Chem. Chem. Phys.* **2010**, *12*, 10329–10340.
(51) Siri, O.; Braunstein, P. *Chem. Commun.* **2002**, 208–209.
(52) Braunstein, P.; Siri, O.; Taquet, J.-P.; Rohmer, M.-M.; Bénard, M.; Welter, R. *J. Am. Chem. Soc.* **2003**, *125*, 12246–12256.
(53) Mansingh, A.; McLay, D. B.; Lim, K. O. *Can. J. Phys.* **1974**, *52*, 2365–2369.
(54) Ishii, H.; Sugiyama, K.; Ito, E.; Seki, K. *Adv. Mater.* **1999**, *11*, 605.
(55) Zhu, X. Y. *Surf. Sci. Rep.* **2004**, *56*, 1.
(56) Balaz, S.; Caruso, A. N.; Platt, N. P.; Dimov, D. I.; Boag, N. M.; Brand, J. I.; Losovyj, Ya. B.; Dowben, P. A. *J. Phys. Chem. B* **2007**, *111*, 7009–7016.
(57) Natan, A.; Kronik, L.; Haick, H.; Tung, R. T. *Adv. Mater.* **2007**, *19*, 4103–4117.
(58) Taguchi, D.; Kajimoto, N.; Manaka, T.; Iwamoto, M. *J. Chem. Phys.* **2007**, *127*, 044703.
(59) Natan, A.; Zidon, Y.; Shapira, Y.; Kronik, L. *Phys. Rev. B* **2006**, *73*, 193310.
(60) Deutsch, D.; Natan, A.; Shapira, Y.; Kronik, L. *J. Am. Chem. Soc.* **2007**, *129*, 2989–2997.
(61) Sushko, M. L.; Shluger, A. L. *Adv. Funct. Mater.* **2008**, *18*, 2228–2236.
(62) Yang, Q.-Z.; Siri, O.; Braunstein, P. *Chem. Commun.* **2005**, 2660–2662.
(63) Yang, Q.-Z.; Siri, O.; Brisset, H.; Braunstein, P. *Tetrahedron Lett.* **2006**, *47*, 5727–5731.
(64) Xu, B.; Choi, J.; Caruso, A. N.; Dowben, P. A. *Appl. Phys. Lett.* **2002**, *80*, 4342–4344.
(65) Xiao, J.; Dowben, P. A. *J. Phys.: Condens. Matter* **2009**, *21*, 052001.
(66) Choi, J.; Borca, C. N.; Dowben, P. A.; Bune, A.; Poulsen, M.; Pebley, S.; Adenwalla, S.; Ducharme, S.; Robertson, L.; Fridkin, V. M.; Palto, S. P.; Petukhova, N.; Yudin, S. G. *Phys. Rev. B* **2000**, *61*, 5760.
(67) Sokolov, A.; Yang, C.-S.; Yuan, L.; Liou, S.-H.; Cheng, R.; Jeong, H.-K.; Komesu, T.; Xu, B.; Borca, C. N.; Dowben, P. A.; Doudin, B. *Europhys. Lett.* **2002**, *58*, 448–454.
(68) Zhang, J.; McIlroy, D. N.; Dowben, P. A.; Zeng, H.; Vidali, G.; Heskett, D.; Onellion, M. *J. Phys.: Condens. Matter* **1995**, *7*, 7185–7194.
(69) McIlroy, D. N.; Zhang, J.; Dowben, P. A.; Heskett, D. *Mater. Sci. Eng., A* **1996**, *217/218*, 64.
(70) Feng, D.-Q.; Wisbey, D.; Losovyj, Ya. B.; Tai, Y.; Zharnikov, M.; Dowben, P. A. *Phys. Rev. B* **2006**, *74*, 165425.
(71) Xiao, J.; Rosa, L. G.; Poulsen, M.; Feng, D. -Q.; Reddy, S.; Takacs, J. M.; Cai, L.; Zhang, J.; Ducharme, S.; Dowben, P. A. *J. Phys.: Condens. Matter* **2006**, *18*, L155.
(72) Choi, J.; Dowben, P. A.; Ducharme, S.; Fridkin, V. M.; Palto, S. P.; Petukhova, N.; Yudin, S. G. *Phys. Lett. A* **1998**, *249*, 505.
(73) Young, J. R. *J. Vac. Sci. Technol.* **1973**, *10*, 212.
(74) Lampe, F. W.; Franklin, J. L.; Field, F. H. *J. Am. Chem. Soc.* **1957**, *79*, 6129.
(75) Ortega, J. E.; Himpsel, F. J.; Li, D.; Dowben, P. A. *Solid State Commun.* **1994**, *91*, 807.
(76) Dowben, P. A. *Surf. Sci. Rep.* **2000**, *40*, 151.
(77) Sato, N.; Seki, K.; Inokuchi, H. J. *J. Chem. Soc., Faraday Trans. II* **1981**, *77*, 1621.
(78) Fukagawa, H.; Yamane, H.; Kataoka, T.; Kera, S.; Nakamura, M.; Kudo, K.; Ueno, N. *Phys. Rev. B* **2006**, *73*, 245310.
(79) Schroeder, P. G.; France, C. B.; Park, J. B.; Parkinson, B. A. *J. Phys. Chem. B* **2003**, *107*, 2253–2261.
(80) Smith, N. V. *Prog. Surf. Sci.* **1988**, *51*, 1227–1294.
(81) Borca, C. N.; Komesu, T.; Dowben, P. A. *J. Electron Spectrosc. Relat. Phenom.* **2002**, *122*, 259–273.